Northeast Journal of Complex Systems (NEJCS)

Volume 5
Number 1 *Special Issue: NERCCS 2023 Papers*

Article 8

June 2023

An Implementation of The Method of Moments on Chemical Systems with Constant and Time-dependent Rates

Emmanuel O. Adara
University of Alabama, Tuscaloosa, eoadara@crimson.ua.edu

Roger B. Sidje
University of Alabama, Tuscaloosa, roger.b.sidje@ua.edu

Recommended Citation

Adara, Emmanuel O. and Sidje, Roger B. (2023) "An Implementation of The Method of Moments on Chemical Systems with Constant and Time-dependent Rates," *Northeast Journal of Complex Systems (NEJCS)*: Vol. 5 : No. 1 , Article 8.
DOI: 10.22191/nejcs/vol5/iss1/8/
Available at: https://orb.binghamton.edu/nejcs/vol5/iss1/8

An implementation of the method of moments on chemical systems with constant and time-dependent rates

Emmanuel Adara[1*] and Roger B. Sidje[1#]

[1] Department of Mathematics, The University of Alabama, Tuscaloosa

[*] eoadara@crimson.ua.edu [#] roger.b.sidje@ua.edu

Abstract

Among numerical techniques used to facilitate the analysis of biochemical reactions, we can use the method of moments to directly approximate statistics such as the mean numbers of molecules. The method is computationally viable in time and memory, compared to solving the chemical master equation (CME) which is notoriously expensive. In this study, we apply the method of moments to a chemical system with a constant rate representing a vascular endothelial growth factor (VEGF) model, as well as another system with time-dependent propensities representing the susceptible, infected, and recovered (SIR) model with periodic contact rate. We assess the accuracy of the method using comparisons with approximations obtained by the stochastic simulation algorithm (SSA) and the chemical Langevin equation (CLE). The VEGF model is of interest because of the role of VEGF in the growth of cancer and other inflammatory diseases and the potential use of anti-VEGF therapies in the treatment of cancer. The SIR model is a popular epidemiological model used in studying the spread of various infectious diseases in a population.

1 Introduction

A chemically reacting system that is both well-stirred and at thermal equilibrium may be viewed as a complex system of particles. In such a system, the particles are molecules (or macromolecules) that can bind or unbind when they randomly collide, triggering the creation, transformation, or destruction of those molecules. Usually in practice, systems are made up of large large quantities of molecules, permitting to track their concentrations through a set of deterministic, nonlinear ordinary different equations (ODEs), commonly referred to as reaction rate equations (RREs).

Of interest to us in this study are the particular contexts, such as within the confine of a biochemical cell, where molecules are only present in small quantities, and where it is more appropriate to retain the fundamentally discrete and stochastic nature of the biochemical processes. Gillespie [6] has demonstrated that the underlying dynamical system in such contexts can be modeled by a continuous-time, discrete state, Markov chain, for which the evolution of the associated probability mass function is governed by the so-called chemical master equation (CME). The reader may also see a very readable overview in the tutorial of Higham [11]. Although originally developed to model simple chemical systems, the same framework has since been successfully applied to more complicated biochemical systems [**?**], despite the fact that some of the assumptions are no longer strictly satisfied – for example in a living cell, the mixture is far from being perfectly homogeneous.

Unfortunately, the CME is difficult to solve, even though it has wide application in biological systems, ecological and pharmacokinetics networks to name a few [10, 9, 14]. Much work has gone into the stochastic simulation of biological system especially in the studying of chemical dynamics [16]. A flagship Monte Carlo method is Gillespie's stochastic simulation algorithm (SSA) [6], which is an exact method of generating sample paths whose (marginal) probability distribution is the solution to the CME [8]. Significant effort has been dedicated over the years to improve the SSA as it can be extremely slow due to the many realizations that need to be averaged to get more accurate approximations of the probability distribution. A few of such improvements include the tau-leaping [3], or slow-scale SSA [2]. Other methods are finite state projection (FSP) [15], adaptive lumping of states [4]. Our manuscript gives a background on the CME in the next section before discussing the moment method and other computational aspects in the following sections.

2 Chemical Master Equation

Assuming the biological system being modeled has N species, say $\{S_1, \ldots, S_N\}$, the dynamical state of the system is defined as the number of copies of each species. Thus at time t, let $\boldsymbol{x}(t) = (x_1(t), \ldots, x_N(t))^T$ be the state vector of nonnegative integers representing the populations, i.e., x_i is the number of copies of species S_i. Each possible configuration of the system defines a distinct vector and so must be interpreted as a state in the Markov chain, thereby defining the state space, which for this class of models, may always be identified with just the N-dimensional lattice of points with nonnegative integer coordinates. But not all configurations are possible (the lattice has "holes" due to reachability issues as illustrated soon).

Species interact via $M \geq 1$ possible chemical reaction channels $\{R_1, \ldots, R_M\}$,

each of the generic form

$$R: \qquad c_1 S_1 + \cdots + c_N S_N \xrightarrow{\kappa} b_1 S_1 + \cdots + b_N S_N, \tag{1}$$

where κ is the reaction rate and the c_i and b_i are, respectively, the coefficients of the *reactants* and *products*.

Transitions between states occur when (and only when) a reaction occurs. For a general reaction of the form (1), there is an associated *stoichiometric vector* $\boldsymbol{\nu} = (b_1 - c_1, \ldots, b_N - c_N)^T$ sized as the state vector and defining how the state changes when the reaction occurs. The components of the stoichiometric vector are integers, recording the increase or decrease in the number of copies of each species after the associated reaction occurs. Specifically, if the system is in state $\boldsymbol{x}$ and reaction j occurs, then the system transitions to state $\boldsymbol{x} + \boldsymbol{\nu}_j$, mimicking a random walk in the N-dimensional lattice. But if $\boldsymbol{x} + \boldsymbol{\nu}_j$ causes a component to become negative, such a reaction cannot happen, suggesting intuitively a "hole" in the lattice as hinted earlier, or formally the notion of reachability in the Markov chain.

As a way of illustrating this background section, suppose we are given a system with three chemical species, S_u, S_v and S_w, that undergo the reaction

$$S_u + S_v \xrightarrow{\kappa_1} S_w \tag{2}$$

The associated stoichiometric vector has -1 in the u^{th} and v^{th} components, and $+1$ in the w^{th} component and is zero elsewhere.

Typically in biological settings only a handful of reaction channels frequently arise. In particular, as well as reaction (2) just mentioned, *birth* (or *immigration*), *death* (or *decay*), and *dimerization* are other common forms. Birth is of the form

$$\emptyset \xrightarrow{\kappa_2} S_u \tag{3}$$

where an instance of a species S_u is gained. The associated stoichiometric vector

$$\boldsymbol{\nu} = (0, \ldots, 0, +1, 0, \ldots, 0)^T$$

has $+1$ in the u^{th} component and is zero elsewhere. Death is the reverse of birth. Dimerization is when two molecules of the same species, called monomers, combine to form a dimer. The chemical reaction is written as

$$2S_u \xrightarrow{\kappa_3} S_v \tag{4}$$

where S_u is the monomer and S_v is the dimer. The associated stoichiometric vector

$$\boldsymbol{\nu} = (0, \ldots, 0, -2, 0, \ldots, 0, +1, 0, \ldots, 0)^T$$

has -2 in the u^{th} component, and $+1$ in the v^{th} component and is zero elsewhere.

It remains only to specify the probability of different kinds of transitions between states, i.e., the relative likelihood of the various reactions. Associated with each state is a set of M *propensities*, $\alpha_1(\boldsymbol{x}), \ldots, \alpha_M(\boldsymbol{x})$, that determine the relative chance of each reaction occurring if the system is in state $\boldsymbol{x}$. The propensities are defined by the requirement that, given $\boldsymbol{x}(t) = \boldsymbol{x}$, then $\alpha_j(\boldsymbol{x})dt$ is the probability of reaction j occurring in the next infinitesimal time interval $[t, t + dt)$, where the dependence on time has now been made explicit. The propensities are state-dependent and have a functional form defined by the stoichiometry of the reaction. For a general reaction (1) under the classic model of mass-action kinetics, the propensity, when in state $\boldsymbol{x}$, is a scaled product of binomial terms:

$$\alpha(\boldsymbol{x}) = \kappa \binom{x_1}{c_1} \binom{x_2}{c_2} \ldots \binom{x_N}{c_N}. \tag{5}$$

Note that (5) does not depend on the products, and the scaling κ is indicative to the fact that not all collisions of the appropriate reactants necessarily result in a reaction. In the case where κ is time-dependent, so too will be the propensities, thus adding a further complexity to the problem.

Assuming the initial probability distribution at $t = 0$ is known, Let $P(\boldsymbol{x}, t)$ be the probability of being in state $\boldsymbol{x}$ at time t, it has been shown to satisfy

$$\frac{\partial P(\boldsymbol{x}, t)}{\partial t} = \sum_{j=1}^{M} \alpha_j(\boldsymbol{x} - \boldsymbol{\nu}_j) P(\boldsymbol{x} - \boldsymbol{\nu}_j, t) - P(\boldsymbol{x}, t) \sum_{j=1}^{M} \alpha_j(\boldsymbol{x}) \tag{6}$$

Equation (6) is what is formally known as the CME, and it can be rewritten as a system of linear ODEs in matrix form:

$$\begin{cases} \boldsymbol{p}'(t) = \boldsymbol{A}\boldsymbol{p}(t) & t \in [0, t_f] \\ \boldsymbol{p}(0) = \boldsymbol{p}_0 & \text{initial condition.} \end{cases} \tag{7}$$

where the state space has been explicitly enumerated, and the probability vector $\boldsymbol{p} = (p_1, p_2, \ldots)^T$ is indexed by the states, i.e., $p_i = P(\boldsymbol{x}_i, t)$ with a state $\boldsymbol{x}_i$ identified just by its index i in the enumeration. The entries of the transition matrix $\boldsymbol{A} = [\alpha_{i,j}]$ are populated with the propensities of transitioning between states j and i. As there are impossible transitions due to unreachability between states, the corresponding entries are zeros, and because there are many of them in practice, $\boldsymbol{A}$ is a large sparse matrix. In the case of constant rates and given an initial probability vector $\boldsymbol{p}_0$ representing the initial condition of the biochemical system, the exact solution at time t is:

$$\boldsymbol{p}(t) = e^{t\boldsymbol{A}} \boldsymbol{p}_0 \tag{8}$$

Naive methods cannot be employed to solve the CME due to the large size of the matrix, or when there are time-dependent rates.

3 Chemical Langevin Equation

The Chemical Langevin equation (CLE) is a set of coupled, nonlinear stochastic differential equations (SDEs) [16] which describes the time evolution of the molecule numbers of each species. The CLE method simulate the stochastic dynamics of chemical systems as it factors in noise, hence, the probability density result to the Fokker-Planck equation, which approximate the chemical master equation solution [17]. The concept, derivation and accuracy of the CLE method in comparison to the SSA and other methods in solving the master equation has been extensively explored in literature [7, 12, 5].

As noted in [16], one of the major setbacks of CLE is that it can break down for systems with small numbers in molecules due to the problem of evaluating square roots of negative quantities.

Denoting the amount of species i at time t by a real-valued random variable $x_i(t)$. for a dynamical system with chemical master equation (6), the chemical Langevin equation [7] is derived thus:

$$\boldsymbol{x}(t+\tau) = \boldsymbol{x}(t) + \tau \sum_{j=1}^{M} \boldsymbol{\nu}_j \alpha_j(\boldsymbol{x}(t)) + \sqrt{\tau} \sum_{j=1}^{M} \boldsymbol{\nu}_j \sqrt{\alpha_j(\boldsymbol{x}(t))} Z_j \tag{9}$$

where, Z_j depict independent normal random variables drawn in $(0, 1)$, $\boldsymbol{x}(t)$ is the state vector in $\mathbb{R}^N$ at time t and τ is the leap time.

4 Method of Moments

As in section 2, let $P(\boldsymbol{x}, t)$ be the probability of being in state $\boldsymbol{x}$ at time t. The mean or first-order moment associated to x_i is defined as

$$\mu_i = \mathbb{E}[x_i] = \sum_{\boldsymbol{x}} x_i P(\boldsymbol{x}, t)$$

but that definition involves knowing $P(\boldsymbol{x}, t)$, which involves the onerous task of solving the CME. The method of moments seeks a work around by multiplying the CME (6) by x_i and summing over all reachable states $\boldsymbol{x} = (x_1, x_2, ..., x_N)^T$

$$\sum_{\boldsymbol{x}} x_i \frac{\partial P(\boldsymbol{x}, t)}{\partial t} \;=\; \sum_{\boldsymbol{x}} \Big[\sum_{j=1}^{M} x_i \alpha_j(\boldsymbol{x} - \boldsymbol{\nu}_j) P(\boldsymbol{x} - \boldsymbol{\nu}_j, t) - x_i P(\boldsymbol{x}, t) \sum_{j=1}^{M} \alpha_j(\boldsymbol{x}) \Big]$$

Following the derivation in [13], it comes

$$\frac{d\mathbb{E}[x_i]}{dt} = \sum_{\boldsymbol{x}} \sum_{j=1}^{M} \nu_{j,i} \alpha_j(\boldsymbol{x}) P(\boldsymbol{x}, t)$$

$$\frac{d\mathbb{E}[(x_i - \mu_i)(x_j - \mu_j)]}{dt} = \sum_{k=1}^{M} \Big(\nu_{k,i} \mathbb{E}[(x_j - \mu_j)\alpha_k(\boldsymbol{x})] + \nu_{k,j} \mathbb{E}[(x_i - \mu_i)\alpha_k(\boldsymbol{x})] + \nu_{k,i}\nu_{k,j} \mathbb{E}[\alpha_k(\boldsymbol{x})] \Big)$$

The equation associated to the second-order moment is derived thus:

$$\frac{\partial \mu_i}{\partial t} = \sum_j \nu_{j,i} \left[\alpha_j(\boldsymbol{\mu}) + \frac{1}{2} \sum_{l,k} \frac{\partial^2 \alpha_j(\boldsymbol{\mu})}{\partial x_l \partial x_k} C_{lk} \right]$$

$$\begin{aligned} \frac{\partial C_{ij}}{\partial t} = \sum_k \Bigg[& \nu_{k,i}\nu_{k,j}\alpha_k(\boldsymbol{\mu}) + \sum_l \frac{\partial \alpha_j(\boldsymbol{\mu})}{\partial x_l} \big(\nu_{k,i} C_{jl} + \nu_{k,j} C_{il} \big) \\ & + \frac{1}{2} \sum_{l,k} \frac{\partial^2 \alpha_j(\boldsymbol{\mu})}{\partial x_l \partial x_k} \big(\nu_{k,i}\nu_{k,j} C_{lk} + \nu_{k,i} C_{jlk} + \nu_{k,j} C_{ilk} \big) \Bigg] \end{aligned}$$

where μ_i and C_{ij} are the mean and covariance respectively. C_{ilk} is the third-order moment of x_i, x_l, and x_k. Since, the i^{th} moment equation depends on $(i+1)^{th}$ moment, hence the third-order moment is expressed in terms of the first and second order moment using appropriate moment closure technique.

5 Numerical Tests

5.1 Constant Reaction Rate:Vascular Endothelial Growth Factor (VEGF) Model

The vascular endothelial growth factor (VEGF) receptor model is a system that describes the events that lead to angiogenesis, the process where new blood vessels are generated from vasculature following the release of growth factors from the surrounding tissue. Growth factors are special types of cytokines, and endothelial cells possess specific receptors, namely the VEGF receptor, to which these growth factors bind.

The model species are represented with U, B, X and L, where U is an unbound receptor, B is a bound receptor, X is an oligomer (a molecular complex containing

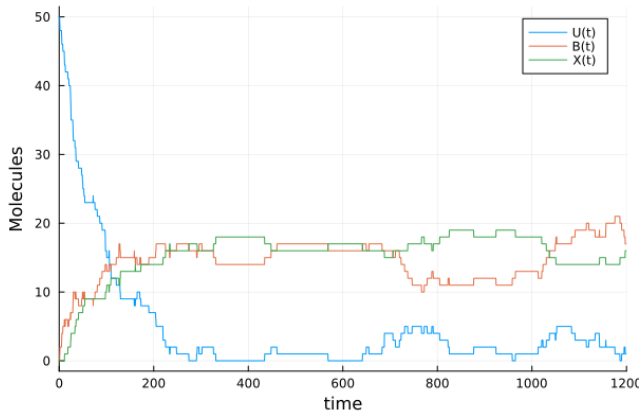

Figure 1: Single realisation of the VEGF model with SSA

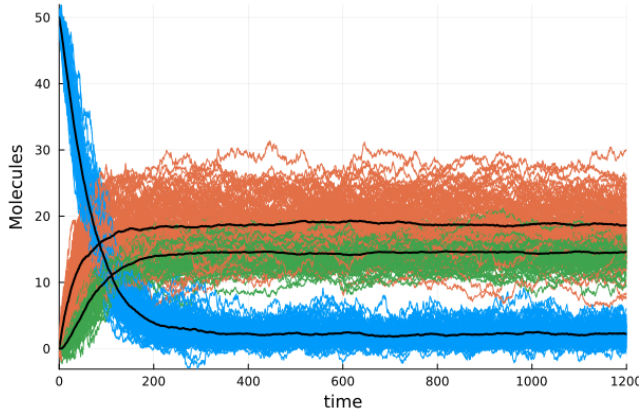

Figure 2: 1000 realisations of the VEGF model with the mean numbers of molecule

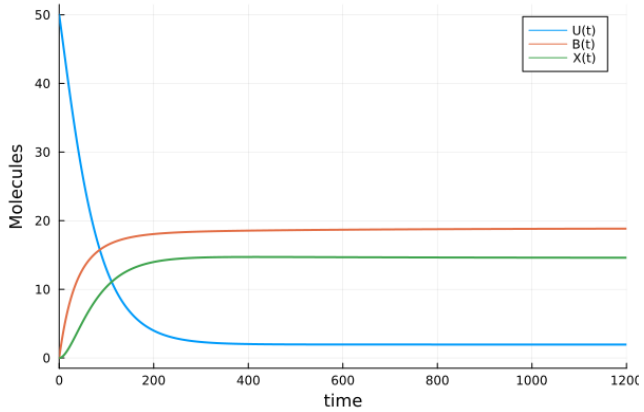

Figure 3: Mean numbers of molecules of the VEGF model generated with the method of moments

Reaction Channels	Propensity
$\mathrm{U} + \mathrm{L} \xrightarrow{k_{on}} \mathrm{B}$	$k_{on}[L][U]$
$\mathrm{B} \xrightarrow{k_{off}} \mathrm{U} + \mathrm{L}$	$k_{off}[B]$
$\mathrm{U} + \mathrm{B} \xrightarrow{k_{on}^X} \mathrm{X}$	$\frac{k_{on}^X \Delta^2 [U][B]}{4R^2}$
$\mathrm{X} \xrightarrow{k_{off}^X} U + B$	$k_{off}^X [X]$

Table 1: Reaction Channels and Propensity of VEGF Receptor Model. The Parameters[1] are $k_{on} = 1.0 \times 10^{-5}, k_{off} = 1.0 \times 10^{-3}, k_{on}^X = 2.304 \times 10^3, k_{off}^X = 1.0 \times 10^{-3}, \Delta = 2.5 \times 10^{-9}, R = 3.0 \times 10^{-6}, L = 1000$

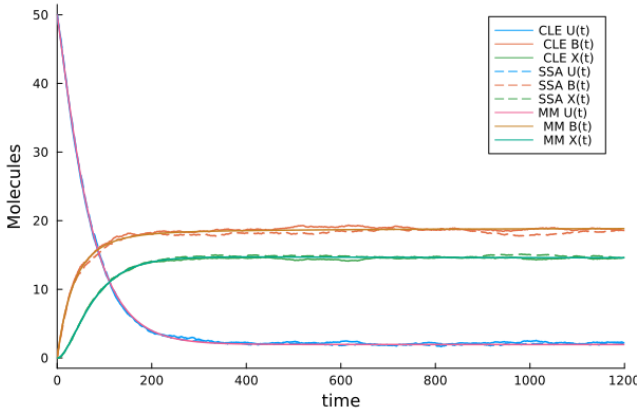

Figure 4: A comparison of the mean number of molecules of the VEGF model using the SSA, CLE and method of moments

few repeating structural units) of receptors and ligand (a molecule that binds to another larger molecule). In this model, L depicts the concentration of free ligand.

Using the initial condition $[U, B, X] = [50, 0, 0]$. The vascular endothelial growth factor (VEGF) receptor model is simulated using the parameters from [1]. Figure 1 shows one realization of the stochastic simulation algorithm (SSA) execution of the model,multiple realisations of the model with the average(mean) number of molecules with respect to time is shown in figure 2.

Figure 3 shows the mean numbers of molecules of $U(t)$, $B(t)$, $X(t)$ by method of moment. Figure 4 shows the mean copy number of VEGF receptors from the three methods under consideration: the Stochastic simulation algorithm (SSA), chemical Langevin equation (CLE), and moment method. It can be seen that the results derived using the moment method agrees with the results obtained using the stochastic simulation algorithm and chemical Langevin equation; that is the moment method

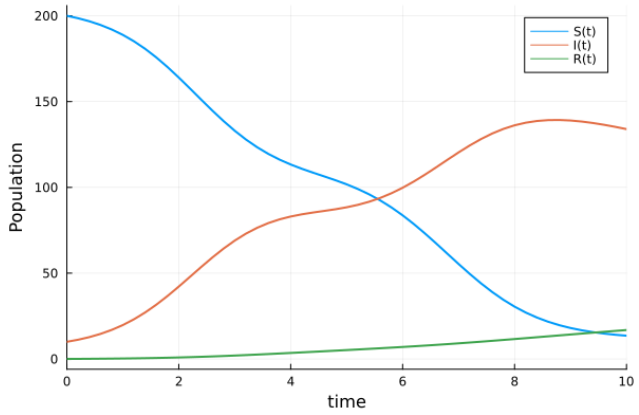

Figure 5: Mean population of the SIR model generated with the method of moments

gives an efficient approximation of the chemical master equation.

5.2 Time-dependent Reaction Rate:SIR Epidemic Model

We considered a three species SIR epidemic model with periodic rate reaction with Susceptible(S), Infected(I) and Recovered(R) population, the reaction channels are given below:

Reaction Channels	Propensity
S + I $\xrightarrow{k_1}$ 2I	$k_1[S][I]$
I $\xrightarrow{k_2}$ R	$k_2[I]$
R $\xrightarrow{k_3}$ S	$k_3[R]$
S $\xrightarrow{k_4}$ $\emptyset$	$k_4[S]$
I $\xrightarrow{k_5}$ $\emptyset$	$k_5[I]$
R $\xrightarrow{k_6}$ $\emptyset$	$k_6[R]$

Table 2: Reaction Channels and Propensity of the SIR model. The Parameters[19] are $k_1 = 0.003f(t), k_2 = 0.02, k_3 = 0.007, k_4 = 0.002, k_5 = 0.05, k_6 = 0.002$

The interaction between the susceptible population and the infected population was modeled with a periodic contact rate $f(t) = (1 + 0.6\sin(\pi t/3))$.
In order to compare the different approaches (SSA, CLE and moments) for the [S I R] population states, we computed with the initial population [200 10 0] over [0 10](years) timeframe.

Figures 5 and 6 shows the mean population of $S(t)$, $I(t)$, $R(t)$ by method of moment and multiple realisations for the SIR model with average population (mean population) respectively. As can be seen in Figure 7, the mean population of the

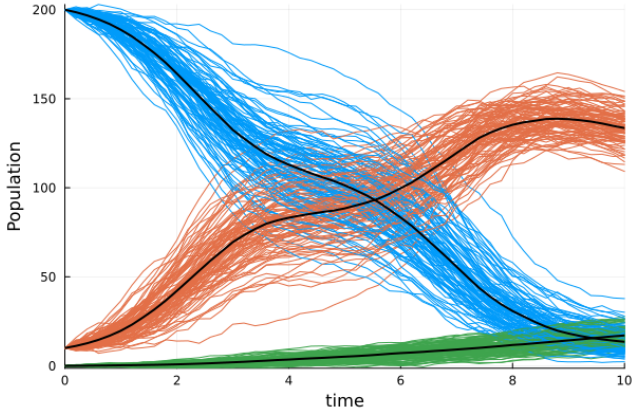

Figure 6: 100 realisations of the SIR Epidemic model with the mean population

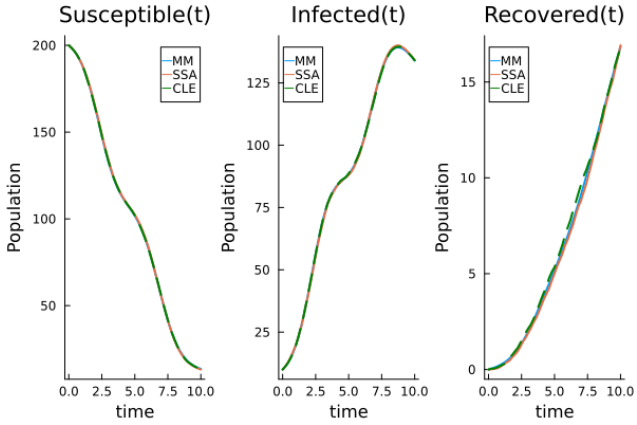

Figure 7: Comparison of the mean population in SIR using the SSA, CLE and moments

periodic epidemic model derived using the moment method agrees with the results obtained using the SSA and CLE; that is the moment method gives an efficient approximation of the chemical master equation.

6 Conclusion

A comparative analysis was carried out on three different methods for approximating the CME solution, namely the SSA, the CLE and the method of moments. The three methods were applied to dynamical systems with constant and and time dependent rates. This work further lend credence to the accuracy and efficiency of the method of moments as a good approximation method for the CME. The method of moment is computationally less demanding (in time and storage) when compared to the SSA and CLE. The setback of the method of moment is the dependence of the resulting moment equation on higher order moments, this can be overcome by using appropriate moment closure method, which involves writing the higher order moments in terms of lower order moments. The presented results agree with literature on the solution of the chemical systems.

References

[1] Tomás Alarcón and Karen M Page. Mathematical models of the vegf receptor and its role in cancer therapy. *Journal of The Royal Society Interface*, 4(13):283–304, 2007.

[2] Yang Cao, Daniel T Gillespie, and Linda R Petzold. The slow-scale stochastic simulation algorithm. *The Journal of chemical physics*, 122(1):014116, 2005.

[3] Yang Cao, Daniel T Gillespie, and Linda R Petzold. Efficient step size selection for the tau-leaping simulation method. *The Journal of chemical physics*, 124(4):044109, 2006.

[4] Lars Ferm and Per Lötstedt. Adaptive solution of the master equation in low dimensions. *Applied numerical mathematics*, 59(1):187–204, 2009.

[5] M. Gibson and J. Bruck. Efficient exact stochastic simulation of chemical systems with many species and many channels. *J. Phys. Chem. A*, 104(9):1876–1889, 2000.

[6] D.T. Gillespie. A rigorous derivation of the chemical master equation. *Physica A*, 188(1-3):404–425, 1992.

[7] D.T. Gillespie. The chemical Langevin equation. *J. Chem. Phys*, 113(1):297, 2000.

[8] D.T. Gillespie and L.R. Petzold. Improved leap-size selection for accelerated stochastic simulation. *J. Chem. Phys*, 119(16):8229, 2003.

[9] John Goutsias and Garrett Jenkinson. Markovian dynamics on complex reaction networks. *Physics reports*, 529(2):199–264, 2013.

[10] Herbert W Hethcote. The mathematics of infectious diseases. *SIAM review*, 42(4):599–653, 2000.

[11] D. J. Higham. Modeling and simulating chemical reactions. *SIAM Review*, 50(2):347–368, January 2008.

[12] Desmond J. Higham. Stochastic ordinary differential equations in applied and computational mathematics. *IMA Journal of Applied Mathematics*, 76(3):449–474, 04 2011.

[13] Chang Hyeong Lee. A moment closure method for stochastic chemical reaction networks with general kinetics. 2013.

[14] Shev MacNamara, Alberto M Bersani, Kevin Burrage, and Roger B Sidje. Stochastic chemical kinetics and the total quasi-steady-state assumption: application to the stochastic simulation algorithm and chemical master equation. *The Journal of chemical physics*, 129(9):09B605, 2008.

[15] Brian Munsky and Mustafa Khammash. The finite state projection algorithm for the solution of the chemical master equation. *The Journal of chemical physics*, 124(4):044104, 2006.

[16] David Schnoerr, Guido Sanguinetti, and Ramon Grima. The complex chemical langevin equation. *The Journal of Chemical Physics*, 141(2):024103, 2014.

[17] Paul Sj berg, Per L tstedt, and Johan Elf. Fokker- planck approximation of the master equation in molecular biology. *Computing and Visualization in Science*, 12(1):37–50, 2009.

[18] Augustinas Sukys and Ramon Grima. MomentClosure.jl: automated moment closure approximations in Julia. *Bioinformatics*, 38(1):289–290, 06 2021.

[19] Vo Hong Thanh and Corrado Priami. Simulation of biochemical reactions with time-dependent rates by the rejection-based algorithm. *The Journal of chemical physics*, 143(5):08B601_1, 2015.

APENDIX

6.1 Moment Equation for SIR Model

Below is the moment equation generated from the SIR Epidemic model with periodic rate,using MomentClosure on Julia [18], the output has been restructured and re-written for readability purpose where $\mu_{100}, \mu_{010}, \mu_{001}$ represents the means, $\mu_{200}, \mu_{020}, \mu_{002}$ represents the variances for the susceptible, infected and recovered population respectively, while the covariance for the SIR populations, i.e $COV(S, I) = \mu_{110},\ COV(S, R) = \mu_{101},\ COV(I, S) = \mu_{011}$

$$\begin{aligned}
\frac{d\mu_{100}}{dt} =& k_3\mu_{001} - k_4\mu_{100} - k_1\mu_{110} - 0.6k_1\mu_{110}\sin\left(\frac{2\pi t}{6}\right) \\
\frac{d\mu_{010}}{dt} =& k_1\mu_{110} + 0.6k_1\mu_{110}\sin\left(\frac{2\pi t}{6}\right) - k_5\mu_{010} - k_2\mu_{010} \\
\frac{d\mu_{001}}{dt} =& k_2\mu_{010} - k_6\mu_{001} - k_3\mu_{001}
\end{aligned}$$

$$\begin{aligned}
\frac{d\mu_{200}}{dt} =& k_1\mu_{110} + k_3\mu_{001} + k_4\mu_{100} + 2k_3\mu_{101} + 0.6k_1\mu_{110}\sin\left(\frac{2\pi t}{6}\right) + 4k_1\mu_{100}^2\mu_{010} \\
&+ 2.4k_1\mu_{100}^2\mu_{010}\sin\left(\frac{2\pi t}{6}\right) - 2k_4\mu_{200} - 2k_1\mu_{010}\mu_{200} - 4k_1\mu_{100}\mu_{110} \\
&- 1.2k_1\mu_{010}\mu_{200}\sin\left(\frac{2\pi t}{6}\right) - 2.4k_1\mu_{100}\mu_{110}\sin\left(\frac{2\pi t}{6}\right) \\
\frac{d\mu_{110}}{dt} =& k_3\mu_{011} + k_1\mu_{010}\mu_{200} + 2k_1\mu_{010}^2\mu_{100} + 2k_1\mu_{100}\mu_{110} + 1.2k_1\mu_{010}^2\mu_{100}\sin\left(\frac{2\pi t}{6}\right) \\
&+ 0.6k_1\mu_{010}\mu_{200}\sin\left(\frac{2\pi t}{6}\right) + 1.2k_1\mu_{100}\mu_{110}\sin\left(\frac{2\pi t}{6}\right) - k_5\mu_{110} \\
&- k_1\mu_{110} - k_2\mu_{110} - k_4\mu_{110} - k_1\mu_{020}\mu_{100} - 0.6k_1\mu_{110}\sin\left(\frac{2\pi t}{6}\right) - 2k_1\mu_{100}^2\mu_{010} \\
&- 2k_1\mu_{010}\mu_{110} - 0.6k_1\mu_{020}\mu_{100}\sin\left(\frac{2\pi t}{6}\right) - 1.2k_1\mu_{100}^2\mu_{010}\sin\left(\frac{2\pi t}{6}\right) \\
&- 1.2k_1\mu_{010}\mu_{110}\sin\left(\frac{2\pi t}{6}\right) \\
\frac{d\mu_{101}}{dt} =& k_3\mu_{002} + k_2\mu_{110} + 2k_1\mu_{001}\mu_{010}\mu_{100} + 1.2k_1\mu_{001}\mu_{010}\mu_{100}\sin\left(\frac{2\pi t}{6}\right) - k_6\mu_{101} - k_3\mu_{001} \\
&- k_3\mu_{101} - k_4\mu_{101} - k_1\mu_{010}\mu_{101} - k_1\mu_{001}\mu_{110} - k_1\mu_{011}\mu_{100} - 0.6k_1\mu_{001}\mu_{110}\sin\left(\frac{2\pi t}{6}\right) \\
&- 0.6k_1\mu_{011}\mu_{100}\sin\left(\frac{2\pi t}{6}\right) - 0.6k_1\mu_{010}\mu_{101}\sin\left(\frac{2\pi t}{6}\right) \\
\frac{d\mu_{020}}{dt} =& k_5\mu_{010} + k_2\mu_{010} + k_1\mu_{110} + 2k_1\mu_{020}\mu_{100} + 4k_1\mu_{010}\mu_{110} + 0.6k_1\mu_{110}\sin\left(\frac{2\pi t}{6}\right) \\
&+ 2.4k_1\mu_{010}\mu_{110}\sin\left(\frac{2\pi t}{6}\right) + 1.2k_1\mu_{020}\mu_{100}\sin\left(\frac{2\pi t}{6}\right) - 2k_5\mu_{020} \\
&- 2k_2\mu_{020} - 4k_1\mu_{010}^2\mu_{100} - 2.4k_1\mu_{010}^2\mu_{100}\sin\left(\frac{2\pi t}{6}\right) \\
\frac{d\mu_{011}}{dt} =& k_2\mu_{020} + k_1\mu_{010}\mu_{101} + k_1\mu_{001}\mu_{110} + k_1\mu_{011}\mu_{100} + 0.6k_1\mu_{001}\mu_{110}\sin\left(\frac{2\pi t}{6}\right) \\
&+ 0.6k_1\mu_{011}\mu_{100}\sin\left(\frac{2\pi t}{6}\right) + 0.6k_1\mu_{010}\mu_{101}\sin\left(\frac{2\pi t}{6}\right) - k_2\mu_{010} - k_5\mu_{011} \\
&- k_6\mu_{011} - k_2\mu_{011} - k_3\mu_{011} - 2k_1\mu_{001}\mu_{010}\mu_{100} - 1.2k_1\mu_{001}\mu_{010}\mu_{100}\sin\left(\frac{2\pi t}{6}\right) \\
\frac{d\mu_{002}}{dt} =& k_6\mu_{001} + k_3\mu_{001} + k_2\mu_{010} + 2k_2\mu_{011} - 2k_6\mu_{002} - 2k_3\mu_{002}
\end{aligned}$$

6.2 Moment Equation for VEGF Model

Using MomentClosure package on Julia [18], the equations for the method of moments generated from the vascular endothelial growth factor(VEGF) model are shown below. In this model, the concentration of free ligand is L is set up as a placeholder molecule, hence the four subscripts in the solutions

$$
\begin{aligned}
\frac{d\mu_{1000}}{dt} =& k_{off}\mu_{0010} + k_{off}^{X}\mu_{0001} - k_{on}\mu_{1100} - 0.25k_{on}^{X}\Delta^{2}R^{-2}\mu_{1010} \\
\frac{d\mu_{0100}}{dt} =& k_{off}\mu_{0010} - k_{on}\mu_{1100} \\
\frac{d\mu_{0010}}{dt} =& k_{on}\mu_{1100} + k_{off}^{X}\mu_{0001} - k_{off}\mu_{0010} - 0.25k_{on}^{X}\Delta^{2}R^{-2}\mu_{1010} \\
\frac{d\mu_{0001}}{dt} =& 0.25k_{on}^{X}\Delta^{2}R^{-2}\mu_{1010} - k_{off}^{X}\mu_{0001} \\
\frac{d\mu_{2000}}{dt} =& k_{off}\mu_{0010} + k_{on}\mu_{1100} + k_{off}^{X}\mu_{0001} + 2k_{off}\mu_{1010} + 2k_{off}^{X}\mu_{1001} + 4k_{on}\mu_{1000}^{2}\mu_{0100} \\
&+ k_{on}^{X}\Delta^{2}R^{-2}\mu_{1000}^{2}\mu_{0010} + 0.25k_{on}^{X}\Delta^{2}R^{-2}\mu_{1010} - 2k_{on}\mu_{0100}\mu_{2000} - 4k_{on}\mu_{1000}\mu_{1100} \\
&- k_{on}^{X}\Delta^{2}R^{-2}\mu_{1000}\mu_{1010} - 0.5k_{on}^{X}\Delta^{2}R^{-2}\mu_{0010}\mu_{2000} \\
\frac{d\mu_{1100}}{dt} =& k_{off}\mu_{0010} + k_{off}^{X}\mu_{0101} + k_{on}\mu_{1100} + k_{off}\mu_{0110} + k_{off}\mu_{1010} + 2k_{on}\mu_{1000}^{2}\mu_{0100} + 2k_{on}\mu_{0100}^{2}\mu_{1000} \\
&+ 0.5k_{on}^{X}\Delta^{2}R^{-2}\mu_{0010}\mu_{0100}\mu_{1000} - k_{on}\mu_{0100}\mu_{2000} - k_{on}\mu_{0200}\mu_{1000} - 2k_{on}\mu_{0100}\mu_{1100} \\
&- 2k_{on}\mu_{1000}\mu_{1100} - 0.25k_{on}^{X}\Delta^{2}R^{-2}\mu_{0010}\mu_{1100} - 0.25k_{on}^{X}\Delta^{2}R^{-2}\mu_{0100}\mu_{1010} \\
&- 0.25k_{on}^{X}\Delta^{2}R^{-2}\mu_{0110}\mu_{1000} \\
\frac{d\mu_{1010}}{dt} =& k_{off}^{X}\mu_{0001} + k_{off}^{X}\mu_{0011} + k_{off}\mu_{0020} + k_{off}^{X}\mu_{1001} + k_{on}\mu_{0100}\mu_{2000} + 2k_{on}\mu_{1000}\mu_{1100} \\
&+ 2k_{on}\mu_{0010}\mu_{0100}\mu_{1000} + 0.25k_{on}^{X}\Delta^{2}R^{-2}\mu_{1010} + 0.5k_{on}^{X}\Delta^{2}R^{-2}\mu_{1000}^{2}\mu_{0010} \\
&+ 0.5k_{on}^{X}\Delta^{2}R^{-2}\mu_{0010}^{2}\mu_{1000} - k_{off}\mu_{0010} - k_{off}\mu_{1010} - k_{on}\mu_{1100} - 2k_{on}\mu_{1000}^{2}\mu_{0100} \\
&- k_{on}\mu_{0100}\mu_{1010} - k_{on}\mu_{0110}\mu_{1000} - k_{on}\mu_{0010}\mu_{1100} - 0.25k_{on}^{X}\Delta^{2}R^{-2}\mu_{0010}\mu_{2000} \\
&- 0.25k_{on}^{X}\Delta^{2}R^{-2}\mu_{0020}\mu_{1000} - 0.5k_{on}^{X}\Delta^{2}R^{-2}\mu_{0010}\mu_{1010} - 0.5k_{on}^{X}\Delta^{2}R^{-2}\mu_{1000}\mu_{1010}
\end{aligned}
$$

$$\begin{aligned}
\frac{d\mu_{1001}}{dt} =& k_{off}\mu_{0011} + k_{off}^{X}\mu_{0002} + 2k_{on}\mu_{0001}\mu_{0100}\mu_{1000} + 0.5k_{on}^{X}\Delta^2 R^{-2}\mu_{1000}\mu_{1010} \\
&+ 0.25k_{on}^{X}\Delta^2 R^{-2}\mu_{0010}\mu_{2000} + 0.5k_{on}^{X}\Delta^2 R^{-2}\mu_{0001}\mu_{0010}\mu_{1000} - k_{off}^{X}\mu_{0001} - k_{off}^{X}\mu_{1001} \\
&- k_{on}\mu_{0001}\mu_{1100} - k_{on}\mu_{0101}\mu_{1000} - k_{on}\mu_{0100}\mu_{1001} - 0.25k_{on}^{X}\Delta^2 R^{-2}\mu_{1010} \\
&- 0.25k_{on}^{X}\Delta^2 R^{-2}\mu_{0010}\mu_{1001} - 0.25k_{on}^{X}\Delta^2 R^{-2}\mu_{0011}\mu_{1000} - 0.5k_{on}^{X}\Delta^2 R^{-2}\mu_{1000}^2\mu_{0010} \\
&- 0.25k_{on}^{X}\Delta^2 R^{-2}\mu_{0001}\mu_{1010} \\
\frac{d\mu_{0200}}{dt} =& k_{on}\mu_{1100} + k_{off}\mu_{0010} + 2k_{off}\mu_{0110} + 4k_{on}\mu_{0100}^2\mu_{1000} - 2k_{on}\mu_{0200}\mu_{1000} - 4k_{on}\mu_{0100}\mu_{1100} \\
\frac{d\mu_{0110}}{dt} =& k_{off}\mu_{0020} + k_{off}^{X}\mu_{0101} + k_{on}\mu_{0200}\mu_{1000} + 2k_{on}\mu_{0100}\mu_{1100} + 2k_{on}\mu_{0010}\mu_{0100}\mu_{1000} \\
&+ 0.5k_{on}^{X}\Delta^2 R^{-2}\mu_{0010}\mu_{0100}\mu_{1000} - k_{off}\mu_{0010} - k_{on}\mu_{1100} - k_{off}\mu_{0110} - k_{on}\mu_{0100}\mu_{1010} \\
&- k_{on}\mu_{0110}\mu_{1000} - 2k_{on}\mu_{0100}^2\mu_{1000} - k_{on}\mu_{0010}\mu_{1100} - 0.25k_{on}^{X}\Delta^2 R^{-2}\mu_{0010}\mu_{1100} \\
&- 0.25k_{on}^{X}\Delta^2 R^{-2}\mu_{0100}\mu_{1010} - 0.25k_{on}^{X}\Delta^2 R^{-2}\mu_{0110}\mu_{1000} \\
\frac{d\mu_{0101}}{dt} =& k_{off}\mu_{0011} + 2k_{on}\mu_{0001}\mu_{0100}\mu_{1000} + 0.25k_{on}^{X}\Delta^2 R^{-2}\mu_{0010}\mu_{1100} + 0.25k_{on}^{X}\Delta^2 R^{-2}\mu_{0100}\mu_{1010} \\
&+ 0.25k_{on}^{X}\Delta^2 R^{-2}\mu_{0110}\mu_{1000} - k_{off}^{X}\mu_{0101} - k_{on}\mu_{0101}\mu_{1000} - k_{on}\mu_{0001}\mu_{1100} - k_{on}\mu_{0100}\mu_{1001} \\
&- 0.5k_{on}^{X}\Delta^2 R^{-2}\mu_{0010}\mu_{0100}\mu_{1000} \\
\frac{d\mu_{0020}}{dt} =& k_{off}\mu_{0010} + k_{on}\mu_{1100} + k_{off}^{X}\mu_{0001} + 2k_{off}^{X}\mu_{0011} + 2k_{on}\mu_{0100}\mu_{1010} \\
&+ 2k_{on}\mu_{0110}\mu_{1000} + 2k_{on}\mu_{0010}\mu_{1100} + k_{on}^{X}\Delta^2 R^{-2}\mu_{0010}^2\mu_{1000} \\
&+ 0.25k_{on}^{X}\Delta^2 R^{-2}\mu_{1010} - 2k_{off}\mu_{0020} - 4k_{on}\mu_{0010}\mu_{0100}\mu_{1000} - k_{on}^{X}\Delta^2 R^{-2}\mu_{0010}\mu_{1010} \\
&- 0.5k_{on}^{X}\Delta^2 R^{-2}\mu_{0020}\mu_{1000} \\
\frac{d\mu_{0011}}{dt} =& k_{off}^{X}\mu_{0002} + k_{on}\mu_{0001}\mu_{1100} + k_{on}\mu_{0101}\mu_{1000} + k_{on}\mu_{0100}\mu_{1001} + 0.25k_{on}^{X}\Delta^2 R^{-2}\mu_{0020}\mu_{1000} \\
&+ 0.5k_{on}^{X}\Delta^2 R^{-2}\mu_{0010}\mu_{1010} + 0.5k_{on}^{X}\Delta^2 R^{-2}\mu_{0001}\mu_{0010}\mu_{1000} - k_{off}\mu_{0011} - k_{off}^{X}\mu_{0001} \\
&- k_{off}^{X}\mu_{0011} - 2k_{on}\mu_{0001}\mu_{0100}\mu_{1000} - 0.25k_{on}^{X}\Delta^2 R^{-2}\mu_{1010} - 0.25k_{on}^{X}\Delta^2 R^{-2}\mu_{0011}\mu_{1000} \\
&- 0.25k_{on}^{X}\Delta^2 R^{-2}\mu_{0010}\mu_{1001} - 0.25k_{on}^{X}\Delta^2 R^{-2}\mu_{0001}\mu_{1010} - 0.5k_{on}^{X}\Delta^2 R^{-2}\mu_{0010}^2\mu_{1000} \\
\frac{d\mu_{0002}}{dt} =& k_{off}^{X}\mu_{0001} + 0.25k_{on}^{X}\Delta^2 R^{-2}\mu_{1010} + 0.5k_{on}^{X}\Delta^2 R^{-2}\mu_{0011}\mu_{1000} + 0.5k_{on}^{X}\Delta^2 R^{-2}\mu_{0010}\mu_{1001} \\
&+ 0.5k_{on}^{X}\Delta^2 R^{-2}\mu_{0001}\mu_{1010} - 2k_{off}^{X}\mu_{0002} - k_{on}^{X}\Delta^2 b^{-2}\mu_{0001}\mu_{0010}\mu_{1000}
\end{aligned}$$